TECHNISCHE MECHANIK, Band 17, Heft 1, (1997), 31-40
Manuskripteingang: 18. Oktober 1996

Numerical Simulation of Stress Stimulated Bone Remodeling

U. Nackenhorst

The ability of living bones to adapt their structure to the stress conditions leads to a long time failure of common hip joint stem endoprostheses. For the simulation of stress adaptive bone remodeling a new stable and efficient finite element procedure is suggested. Numerical studies based on a two-dimensional model of the femur show the usefulness for a better understanding of bone remodeling. Recommendations for improvements of prosthesis design are derived from these first studies.

1 Introduction

The replacement of human skeleton joints by artificial substitutes is a well established procedure in orthopaedics surgery. The hip joint endoprosthetics plays a major role with a part of approximately 70% of all artificial joint replacements. The total amount of anual hip joint endoprosthetics is estimated to be 200.000 operations throughout the world (Smolinski and Rubash, 1992).

The major problem of the commonly implanted stem endoprostheses is the limited life time which is prognosticated, of about 10 to 15 years. After this time the fixation of the prosthesis stem in the femural bone will be lost for a significant part of patients. And above everything, the life time of a re-implantation is estimated only half of its former endoprosthesis from which it follows that a third or fourth replacement does not make much sense. Because both, cemented and non-cemented prostheses display this long time behavior the ability of the living bone to adapt to the changed loading conditions is assumed to be the main reason for the failures.

The capability of the bone to adapt its architecture onto the loading conditions has led to an optimized light weight structure as shown in Figure 1. Makroscopically the composition is devided into two major regions of material disposition: the cortical bone of the diaphysis and the spongious trabecular oriented bone near the epiphysis. The mechanical task of the trabecular system is to provide a smooth load transfer from the joint into the cortical tube. The cortical bone is a rigid structure with high material density. The spongious bone is built as a framework of rods, the density and orientation of these rods is strictly related to the mechanical demand as shown by Pauwels (1965).

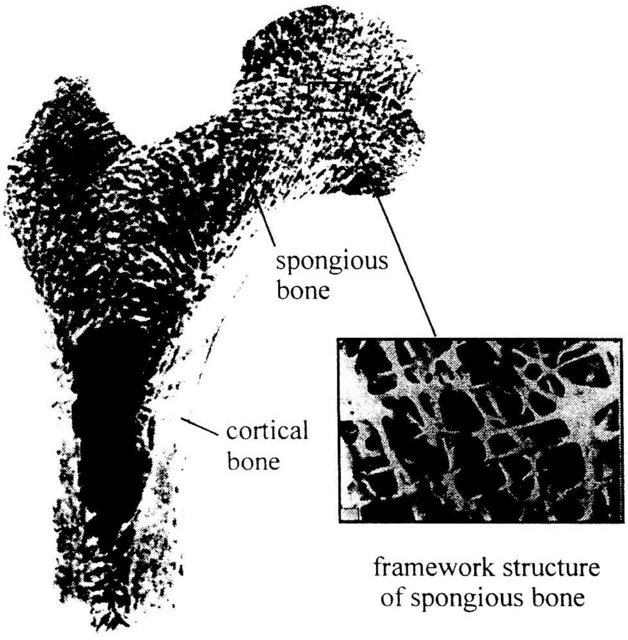

Figure 1. Structure of a Femural Bone

Due to a hip joint replacement this wonderful building is destroided by cutting of the femural head and implanting a stiff artificial structure. The result is a totally changed stress distribution in the remaining bone which induces bone remodeling surrounding the prosthesis. But there are no genetic rules present which provide a long time fixation of the artificial part.

The capability of bones to adapt to changing loading conditions has been well known for more than one century. Wolff (1892) stated his law of transformation, which might be summarized as follows: *Changing working conditions will lead to definite changes of the shape and the internal architecture of bones.*

A couple of theories have been developed to describe the stress adaptive growth of bones. A simple cubic equation has been stated by Kummer (1972), which describes resorption and adsorption depending of the local stress value. Later in the 80's more detailed and complicated models have been published. Guzelsu and Saha (1984) for example explained the remodeling based on the piezoelectric behavior of bones. Hart, Davy and Heimple (1984) presented a cell-activity theory. Besides the mechanical stress there are included genetic, metabolic and hormonal influences. These models are very complicated and include a lot of parameters which have to be specified experimentally before numerical simulations can start.

At the beginning of the 90's simplified theories based on stress only have been used for numerical bone remodeling simulation. Carter and coworkers (Beaupre, Orr and Carter, 1990; Carter, Orr and Fyhrie,1989) suggested a constitutive law $\rho = f(\sigma)$ which relates the material density to the mechanical stress. The stress is calculated by the finite element method (FEM). By use of a two-dimensional finite element model during an iterative procudure the typical characteristics of a femur have been calculated. Weinans, Huiskes and coworkers (Weinans et.al., 1991; van Rietbergen et.al., 1993; Weinans et.al., 1994) used a theory of evolution, e. g. $\dot{\rho} = f(W)$, which relates the velocity of growth with the local strain energy density. The strain energy density for characteristic loading conditions is computed by FEM. By the usage of two- and three-dimentional FE-models the bone remodeling surrounding hip joint prostheses has been simulated. From the biological point of view this theory of evolution seems to be more trust-worthy, but the finite element procedure used by these authors is not very efficient and shows tendencies to lose stability as discussed in Weinans et.al. (1992) and Jacobs et.al. (1995). For a more detailed historical review of bone remodeling theories see Smolinski and Rubash (1992).

Therefore, the theoretical part of this work is addressed to the development of a conditionable stable finite element algorithm for the computation of the nonlinear bio-mechanical interaction probleme of stress adaptive bone remodeling. The practicability of this algorithm will be demonstrated by numerical studies of bone remodeling after hip joint replacement by stem endoprostheses.

2 Theoretical Framework

Evolutional Theory of Bone Remodeling

Similar to the work of Weinans and Huiskes a simple equation of evolution

$$\dot{\rho} = k\left(\frac{W}{W_{\mathrm{ref}}} - 1\right) \tag{1}$$

is used for stress adaptive bone remodeling. Herein $\dot{\rho}$ is the growing speed of the material density. From equation (1) material is added when the strain energy density W is larger than a reference value W_{ref} (adsorption), otherwise the material density decreases (resorption). The parameter k is a time constant of growth describing the physical time scale.

From experiments the relation

$$E = E_0\left(\frac{\rho}{\rho_0}\right)^n \tag{2}$$

between Young's moduls E and material density ρ has been found (Carter and Hayes, 1977), the constants n, E_0 and ρ_0 have been measured as $n = 3$ and $E_0/\rho_0^3 = 3790 \cdot 10^9\ \mathrm{m^8/kg^2\,s^2}$.

From equation (2) there follows that the strain energy density is depending on the actual material density and the mechanical strain ε as well,

$$W(\rho,\varepsilon) = \frac{1}{2\rho}\,\varepsilon^T \mathbf{C}(\rho)\,\varepsilon \tag{3}$$

where $\mathbf{C}$ is the matrix of linear elasticity. For the computational algorithm it is useful to divide W into a pure density dependent and a strain dependent part, i. e.

$$W(\rho,\varepsilon) = \frac{1}{2\rho}\frac{E(\rho)}{E_0}\varepsilon^T \mathbf{C}_0\,\varepsilon = \frac{1}{\rho}\frac{E(\rho)}{E_0}\overline{U} \tag{4}$$

where $\overline{U}$ is the strain energy projected onto a particle of initial density.

In the following, a nondimensional density variable is introduced by scaling the material density.

$$\lambda = \frac{\rho}{\rho_0} \tag{5}$$

Now the equation of evolution is written in a nondimensional form.

$$\dot{\lambda} = k\left(\lambda^{n-1}\frac{\overline{U}}{U_{\text{ref}}} - 1\right) = k\,S \tag{6}$$

where λ may vary between $\lambda_{\min} \approx 0$ and $\lambda_{\max}$ corresponding to the material density of cortical bone. The expression in parenthesis is abbreviated as S, called mechanical stimulus for bone remodeling, herein the abbreviation $U_{\text{ref}} = 2\,\rho_0\,W_{\text{ref}}$ is used.

Time Discretization and Linearization

The integration of the equation (6) of evolution is performed numerically by a time step procedure. For a robust and efficient algorithm an implicit Euler formula has been chosen.

$$\Delta\lambda = k\;{}^{t+\Delta t}S\;\Delta t = {}^{\tau+\Delta\tau}S\;\Delta\tau \tag{7}$$

where

$${}^{\tau+\Delta\tau}S = {}^{\tau+\Delta\tau}\lambda^{n-1}\,\frac{{}^{\tau+\Delta\tau}\overline{U}}{U_{\text{ref}}} - 1 \tag{8}$$

The left superscript denotes the time, where the configuration at time t is known and the configuration at time $t+\Delta t$ has to be computed in the actual time step Δt. Because the coefficient k is not known, the non-dimensional time $\tau = k\,t$ has been introduced.

Taking the nonlinearities into account a consistent linearization has to be performed.

$${}^{\tau+\Delta\tau}S \approx {}^{\tau}S + D_\lambda\left({}^{\tau}S\right)\cdot\Delta\lambda + D_\varepsilon\left({}^{\tau}S\right)\cdot\Delta\varepsilon \tag{9}$$

where $D_z\,(...)$ is the directional derivative with respect to the variable z. This leads to the expression

$${}^{\tau+\Delta\tau}S \approx {}^{\tau}\lambda^{n-1}\frac{{}^{\tau}\overline{U}}{U_{\text{ref}}} - 1 + (n-1)\;{}^{\tau}\lambda^{n-2}\frac{{}^{\tau}\overline{U}}{U_{\text{ref}}}\,\Delta\lambda + {}^{\tau}\lambda^{n-1}\frac{{}^{\tau}\overline{\sigma}}{U_{\text{ref}}}\,\Delta\varepsilon \tag{10}$$

where ${}^{\tau}\overline{\sigma} = \mathbf{C}_0\,{}^{\tau}\varepsilon$ is the stress tensor at time τ projected onto the initial material configuration.

Weak Formulation and Finite Element Approximation

Because it is not possible to derive an analytical solution of the coupled nonlinear bio-mechanical interaction of bone remodeling for arbitrary geometries and boundary conditions it is approximated by use of the finite element method. Foundation of modern finite element theory is a weak formulation, i. e. the formulation of the problem in a variational sense. Therefore, equation (10) is multiplied by a weighting function $\delta\lambda$ and integrated over the volume of the bone *(B)*, which leads to

$$-\int_{(B)}\delta\lambda\;{}^{\tau}\lambda^{n-1}\frac{{}^{\tau}\overline{\sigma}^T}{U_{\text{ref}}}\Delta\tau\,\Delta\varepsilon\,\mathrm{d}V + \int_{(B)}\delta\lambda\left(1-(n-1)\;{}^{\tau}\lambda^{n-2}\frac{{}^{\tau}\overline{U}}{U_{\text{ref}}}\right)\Delta\tau\,\Delta\lambda\,\mathrm{d}V = \int_{(B)}\delta\lambda\;{}^{\tau}S\,\Delta\tau\,\mathrm{d}V \tag{11}$$

In the same manner the equation of mechanical equilibrium has to be prepared, whose weak form is written as

$$\int_{(B)} \rho\, \delta\, {}^{\tau+\Delta\tau}W \, dV - \int_{\partial_t(B)} \delta \mathbf{u}^T \, {}^{\tau+\Delta\tau}\mathbf{t} \, dA = 0 \tag{12}$$

Similar to equation (8) equation (12) has to be linearized with respect to the material density and the mechanical strain. Additionally, it is scaled by the value U_{ref} to get a well posed set of equations, which leads to

$$\frac{1}{U_{\mathrm{ref}}} \int_{(B)} \delta \varepsilon^T \, {}^{\tau}\lambda^n \, \mathbf{C}_0 \, \Delta\varepsilon \, dV + \frac{1}{U_{\mathrm{ref}}} \int_{(B)} \delta \varepsilon^T n \, {}^{\tau}\lambda^{n-1} \, {}^{\tau}\bar{\sigma} \, \Delta\lambda \, dV$$

$$= \frac{1}{U_{\mathrm{ref}}} \int_{\partial_t(B)} \delta \mathbf{u}^T \, {}^{\tau+\Delta\tau}\mathbf{t} \, dA - \frac{1}{U_{\mathrm{ref}}} \int_{(B)} \delta \varepsilon^T \, {}^{\tau}\lambda^{n-1} \, {}^{\tau}\bar{\sigma} \, dV \tag{13}$$

Now equations (11) and (13) describe the bio-mechanical interaction in a variational formulation. For the computation of an approximate solution a finite element discretization is performed by stating an approximation of the displacement and the density field, i. e.

$$\begin{aligned} \mathbf{u}(x,\tau) &= \mathbf{H}(x)\, \hat{\mathbf{u}}(\tau) \\ \lambda(x,\tau) &= \mathbf{G}(x)\, \hat{\lambda}(\tau) \end{aligned} \tag{14}$$

A standard procedure leads to the mixed finite element equation of equilibrium

$$\begin{bmatrix} \mathbf{K}_{uu} & \mathbf{K}_{u\lambda} \\ \mathbf{K}_{\lambda u} & \mathbf{K}_{\lambda\lambda} \end{bmatrix} \begin{bmatrix} \Delta\hat{\mathbf{u}} \\ \Delta\hat{\lambda} \end{bmatrix} = \begin{bmatrix} \hat{\mathbf{f}}_e - \hat{\mathbf{f}}_i \\ \hat{\mathbf{s}} \end{bmatrix} \tag{15}$$

Equation (15) has to be solved within the time step algorithm as long as no incremental changes $\Delta\hat{\mathbf{u}}$ and $\Delta\hat{\lambda}$ appear. Thus, the first row describes the mechanical equilibrium of external nodal forces $\hat{\mathbf{f}}_e$ and internal nodal forces $\hat{\mathbf{f}}_i$. The second row represents the biological equilibrium $(\dot{\lambda} = 0)$, i. e. no bone growth appears anywhere in the structure.

Finite Element Description

For the bone remodeling simulations discussed below a simple hybrid plane stress element has been used. The displacement field is approximated by bilinear shape functions whereas the density field is approximated by constant shape functions. This enables one to eliminate the density variable $\hat{\lambda}$ on element level. But nevertheless, the mechanical stimulus (equation (6)) which reflects in the right hand side $\hat{\mathbf{s}}$ from equation (15) is computed based on a C^0-continuous distribution of the strain energy density. This is necessary to avoid a checker board pattern in the calculated density distribution as discussed by Jacobs et.al. (1995).

A simple superconvergent projection has been used to compute this C^0-continuous strain energy density distribution from the derivatives of the displacement field. By stating

$$\tilde{W} = \mathbf{H}_W \hat{\mathbf{W}} \tag{16}$$

where $\mathbf{H}_W$ are the continuous shape functions (bilinear in this case) and $\hat{\mathbf{W}}$ are the nodal values of the strain energy density, within a weighted residual procedure

$$\int_{(B)} \mathbf{H}_W^T \left(\mathbf{H}_W \hat{\mathbf{W}} - W \right) dV = 0 \tag{17}$$

the projection equation

$$\int_{(B)} \mathbf{H}_W^T \mathbf{H}_W \, dV \; \hat{\mathbf{W}} = \int_{(B)} \mathbf{H}_W^T W \, dV \tag{18}$$

is obtained to compute the nodal values $\hat{\mathrm{W}}$ of the C^0-continuous strain energy density field $\tilde{\mathrm{W}}$. It is remarkable that the right hand side of equation (18) has to be computed with the superconvergent derivatives W, i.e. W has to be computed at the so called superconvergent points in the interior of the elements. Otherwise the projection will be inaccurate as shown by Nackenhorst (1995).

3 Bone Remodeling Simulation

Basis of the stress adaptive bone remodeling simulations discussed in this section is a two-dimensional finite element model of the femur. This geometrical approximation is caused by the very poor knowledge about real three-dimensional loading due to the muscles. Additionally, the material behaviour of the bone is assumed to be isotropic and linearly elastic, because data for a more realistic material description are not available. For this reasons it should be obvious, that the results obtained are not accurate in the sense that they will reflect the realistic behaviour within limited error boundaries. But they will give us an idea of what happens with the bone after endoprosthetics. And the study of parameter variations will allow statements for tendentious improvements.

The 2D Finite Element Model

The finite element meshes used for the simulations are shown in Figure 2. Left the discretization of the physiological femur consisting of 1162 hybrid elements is plotted. In the right the model of the implanted femur is shown, where the elements of the prosthesis are shaded. In the middle the so called side-plate (compare Weinans et.al., 1994) is depicted. This side-plate is superimposed to the bones meshes to ensure a mechanical behaviour close to reality. It does not take place on the bone remodeling process, the material properties are from cortical bone.

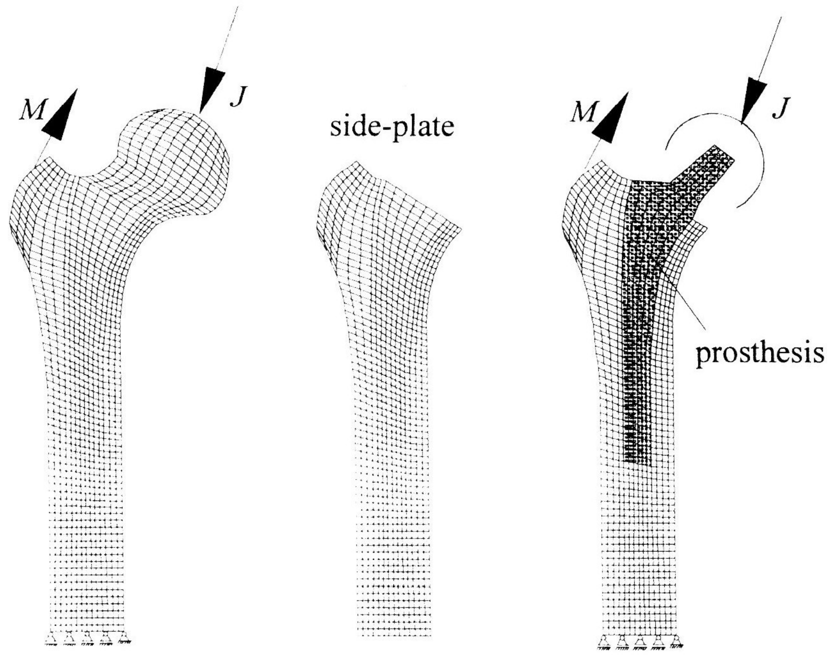

Figure 2. 2D-Finite Element Models for Bone Remodeling Simulation. Left: Physiological Model of a Femural Bone, Middle: Side-plate, Right: Model of an Implanted Femur.

The thickness of all elements is related to the corresponding three-dimensional cross section for both, the bone and the sideplate, to provide a good representation of the 3d-stress state. The loading is approximated from Pauwels one-leg-stand conditions where the resulting forces J and M are applied as distributed loads to the model.

The simulation starts with a homogeneous model of the physiological femur. The initial material properties are described by $\lambda_0 = 1$ to which an initial Young's modulus $E_0 = 2\,\text{GPa}$ is related from equation (2). The physical limits are given by $0.05 \le \lambda \le 2$. The upper limit describes cortical bone ($E_C \approx 16$ GPa). The lower limit is not set to zero for numerical reasons, but the related stiffness of $E_{\min} = 0.25\,\text{MPa}$ is negligible. The Poission ratio has been chosen to be $\nu = 0.29$ which is not changed during the remodeling. The parameter W_{ref} has been obtained to $W_{ref} = 8 \cdot 10^{-3}\,\text{Nm} / \text{kg}$. All computations have been performed with a time increment of $\Delta\tau = 0.02$ which has led within 60 to 200 time steps to a bio-mechanical equilibrium state in the sense of equation (15).

Computation of a Physiological Like Bone Architecture

Starting from a homogeneous density distribution $\lambda_0 = 1$ a close to realistic architecture of the femur has been computed within 60 incremental steps. Figure 3 shows the computed density distribution in comparison with a radiograph of a natural femur. A surprisingly good correlation is observed keeping in mind the simplified model. During this simulation process the cortical walls of the diaphysis and the trabecular structure of the proximal femur have been built up which is in good agreement with the natural bone. Clearly marked are the primary trabecular system (compression) and the secondary arcuate trabecular system (tension). Also the regions of low material density, especially the socalled Ward's triangle, come out very realistically.

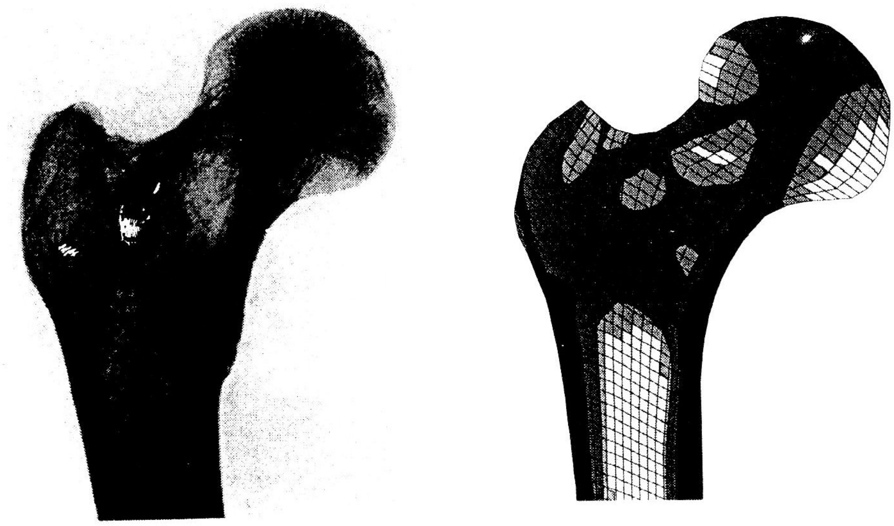

Figure 3. Comparison of the Computed Material Density Distribution with a Radiograph.

Bone Remodeling after Artificial Hip Joint Replacement

To get a better understanding of bone remodeling after hip joint replacement studies with different stem endoprostheses have been carried out. For these studies the geometry (length and width of the stem) and the material properties have been varied. The thickness of the plane stem is 10 mm and constant along its length. An overview of these variations is given in Table 1. The different models are assigned by abbreviations such as *tnl* for a prosthesis of titanium with a narrow and long stem or *sws* for a prosthesis of steel with a width and short stem.

Material	Titanium $E = 110$ GPa, $\nu = 0.29$				Steel $E = 200$ GPa, $\nu = 0.29$	
stem width	11 - 28 mm		15 - 32 mm		15 - 32 mm	
stem length	140 mm	95 mm	140 mm	95 mm	140 mm	95 mm
abbreviation	*tnl*	*tns*	*twl*	*tws*	*swl*	*sws*

Table 1. Variations of Stem Endoprostheses Models

These different endoprosthesis models have been "implanted" into the density distribution presented in the former section. The results of the remodeling simulation will be compared at a defined simulation time after 150 time steps.

The remodeling caused by the *tnl* - prosthesis is shown in Figure 4. Here the density distributions at time step 0 (postoperational) and at time step 150 (long time behaviour) are compared. Because of their small width the narrow prostheses models do not fill out the diaphysis and therefore, the primal fixication is limited to the upper third of their stem.

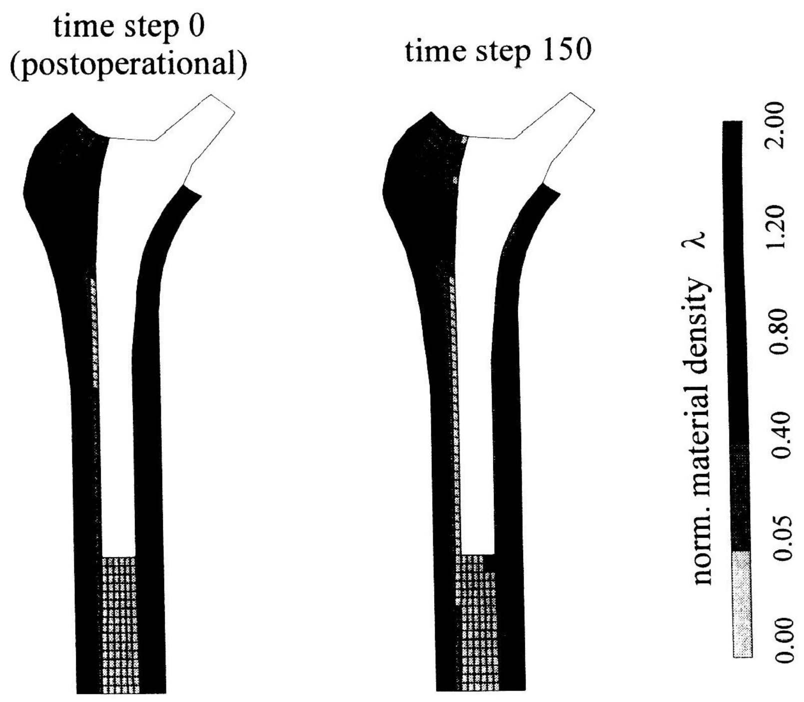

Figure 4. Bone Remodeling Caused by the *tls*-Prosthesis Model

It is remarkable that the bone very quickly shows tendencies to fix the end of the prosthesis stem. Additionally, bone remodeling occurs in the proximal bone. A loss of material density is observed in the medial cortical wall and the trabecular structure of the spongious bone has changed. These bone reactions are in good agreement with clinical observations.

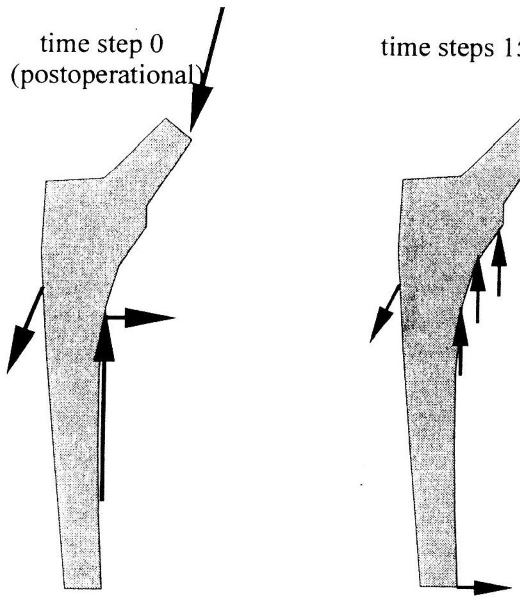

Figure 5. Free-body Diagrams of the Prosthesis Showing the Interaction Forces

The changes of bone structure involve changes of load transfer between prosthesis and bone. An analysis of the corresponding stress states has led to the simplified sketches in Figure 5 showing the mean interaction forces between bone and prosthesis. Postoperational the forces are transmitted mainly at two points because the bone facilitates support only by its existing structure. This geometrically very poor configuration leads to large interaction forces. The bone's reaction to this uncomfortable situation is very intelligent, it tries to fix the tip of the prosthesis stem resulting into a more suitable geometry of the acting forces. Furthermore, the load transfer at the medial side of the proximal third is smoothed. The remaining trabecular structure of the spongious bone now mainly supports the muscle force acting at the trochanter major.

In Figure 6 the resulting density distributions after 150 time steps of four other prosthesis variants are compared. From this comparison follows that obviously the width prosthesis types lead to a principally different remodeling than the narrow ones independent of the material properties and the length of the stem. This is caused by the different initial conditions, the width prosthesis are over their full length in contact with the bone initially which provides a smooth load transfer. But what seems to be good in the beginning will be harmful later. Because the bone is not suitably stressed due to this conditions (*stress shielding*) resorption or a loss of material density occurs in the medial cortical wall. This resorption is the stronger the stiffer the prosthesis shaft is built (compare *twl* and *swl*). Common to all prosthesis models studied here is the reaction of the bone at the end of the stem. In this region the bone is stimulated to adsorption and to fix the tip of the prosthesis.

These first studies of stress adaptive bone remodeling around hip joint stem endoprostheses already allow some recommendations for a more compatible prosthesis design. It seems not to be good to provide a fixation of the stem over its whole length as is common practice with cemented prosthesis systems. This will lead to stress shielding and results in a loss of cortical density. The studies have shown that the rigid contact only in the proximal third as it is usually provided with uncemented prostheses systems will lead to much less resorption. But here the initial geometry of the interaction forces leads to high local stresses. Thus, it seems to be advantageous to fix the tip of the stem a priori to help the bone to adapt to the new situation.

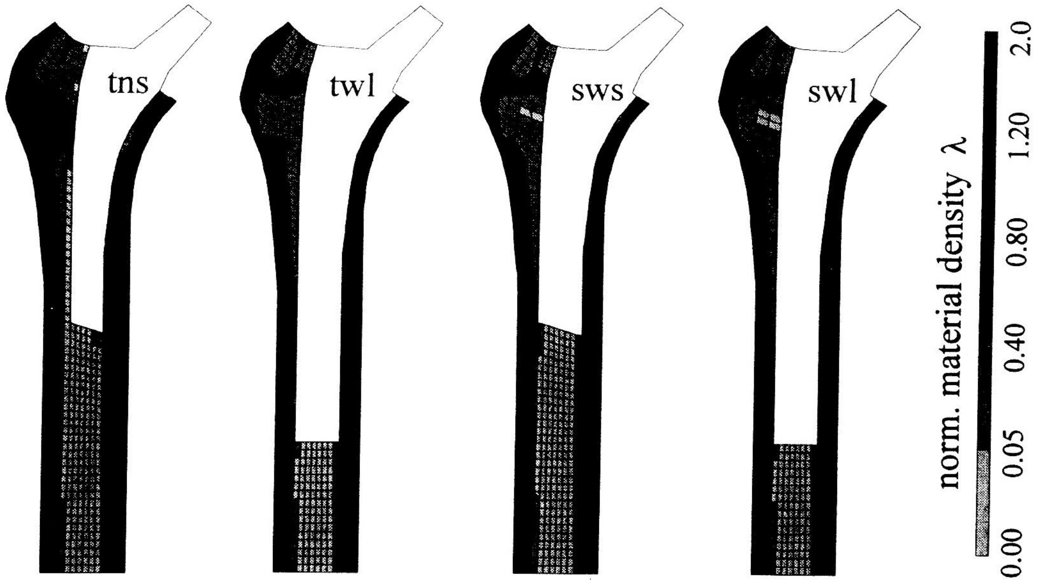

Figure 6. Comparison of the Long Time Configuration Resulting from Different Prostheses Models.

4 Conclusions

A new and efficient finite element procedure for the simulation of stress adaptive bone remodeling has been presented. It is based on a simple theory of evolution which describes the bone growth depending on the local stress state in a continuum sense. The coupling with the mechanical equilibrium equations lead to a consistent formulation of the bio-mechanical interaction problem. A simple hybrid finite element approximation has been chosen for the numerical simulation. Herein, the projection of superconvergent derivatives has been used to avoid known instabilities.

Based on a two-dimensional finite element model of a femur numerical studies have been carried out to understand the bone remodeling after artificial hip joint replacement. The bone remodeling computed from different models of stem endoprostheses has been compared. Already these early studies based on very simple models lead to some recommendations for improved prosthesis designs and surgery techniques.

The expansion of the procedure to three-dimensional simulations including more realistic nonlinear material descriptions and more detailed laws of evolution in addition is easily carried out. But the problem will be the determination of the model parameters, especially the three-dimensional loading conditions due to the muscles. Since those data are missing there will be only a limited progress by three-dimensional simulations aquired with much more manual effort in discretizing and judging the results. But nevertheless, those studies will allow the comparison of realistic prosthesis geometries even today, and the suggested simulation procedure will be an efficient tool for this.

Literature

1. Beaupre; G.; Orr, T.; Carter, D. R.: An Approach for Time Dependent Bone Modeling and Remodeling - Theoretical Development, J. Orthopedic Research, 8, (1990), 651-661

2. Carter, D. R.; Hayes, N. C.: The Behavior of Bone as a Two-phase Porous Structure, J. Bone Joint Surgary, 59, (1977), 954-962

3. Carter, D. R.; Orr, T. E.; Fyhrie, D. P.: Relationships between Loading History and Femural Cancellous Bone Architecture, J. Biomechanics, 22, (1989), 231-244

4. Guzelsu, N.; Saha, S.: Electro-mechanical Behavior of Wet Bone, J. Biomechanics, 106, (1984), 249

5. Hart, R. T.; Davy, D. T.; Heiple, K. G.: Mathematical Modeling and Numerical Solutions for Functionally Dependent Bone Remodeling, Calcif. Tissue Int., 36, (1984), 104

6. Jacobs, C. R.; Levenston, M. E.; Beaupre, G. S.; Simo, J. C.; Carter, D. R.: Numerical Instabilities in Bone Remodeling Simulations: The Advantages of a Node-based Finite Element Approach, J. Biomechanics, 28, (1995), 449-459

7. Nackenhorst, U.: Verbesserte Fehlerschätzverfahren für adaptive Finite Element Analysen in der Elastostatik, in: Nackenhorst, U. (Hrsg.), Technische Mechanik in Forschung und industrieller Praxis, Bericht aus dem Institut für Mechanik der Universität der Bundeswehr Hamburg, Heft August (1996), 191-212

8. Pauwels; F.: Gesammelte Abhandlungen zur funktionellen Anatomie des Bewegungsapparates, Springer-Verlag, Berlin, Heidelberg, New York, (1965)

9. van Rietbergen, B.; Huiskes, R.; Weinans, H.; Sumner, D. R.; Turner, T.M; Galante, J.O.: The Mechanism of Bone Remodeling and Resorption Around Press-Fitted THA Stems, J. Biomechanics, Vol. 26, 4/5, (1993), 369-382

10. Smolinski, P.; Rubash, H. E.: Bone Remodeling Around Hip Implants, Critical Reviews in Biomedical Engineering, 20, 5/6, (1992), 461-483

11. Weinans, H.; Huiskes, R.; Grootenboer, H. J.: The Behavior of Adaptive Bone-Remodeling Simulation Models, J. Biomechanics, 20, 12, (1992), 1425-1441

12. Weinans, H.; Huiskes, R.; Grootenboer, H. J.: Effects of Fit and Bonding Characteristics of Femoral Stems on Adaptive Bone Remodeling, J. Biomechanical Engineering, 116, (1994), 393-400

13. Weinans, H.; Huiskes, R.; Verdonschot, N.; Van Rietbergen, B.: The Effect of Adaptive Bone Remodeling Threshold Levels on Resorption Around Noncemented Hip Stems, Advances in Bioengineering, 20, (1991), 303-306

14. Wolff, J.: Das Gesetz der Transformation der Knochen, Hirschwald, Berlin, (1892)

Address: Dr.-Ing. U. Nackenhorst, University of the Federal Armed Forces, D-22039 Hamburg, Germany